The Fundamentals of Forming Microbubbles in Liquid Metal Systems

Roderick I.L. Guthrie, Mihaiela M. Isac, and Roger T. Ren

Abstract

Gases are now widely used for stirring purposes in liquid metals, given the inventions of the porous plug, as well as other submerged gas injection methods, such as through nozzles, or tuyeres. Nonetheless, we know that any small bubbles forming at the exit pores of porous plugs, will normally rapidly coalesce into much larger bubbles. So, the question of how to form, and maintain, microbubbles in liquid metal systems still remains something of a question. It is nevertheless possible, but only under well-defined conditions. Given that such micro-bubbles can be very helpful in promoting mass transfer reactions (e.g. hydrogen degassing of liquid aluminum), and efficiently removing micro-inclusions (e.g. from liquid steel or aluminium), this is an important topic that needs to be properly addressed. We demonstrate the necessary conditions for the formation of microbubbles, and for their continued existence, by way of a typical ladle-tundish metallurgy example.

Keywords

Microbubbles • Liquid metals • Gas injection

Introduction

Bubbles forming in liquid metals tend to be large compared with the sizes forming in equivalent water models. Their sizes are typically in the oblate spheroid ($\sim$1–10 mm equivalent diameter, D_e, range), or the even larger spherical cap (D_e = 10–100 mm equivalent diameter) range. These large bubbles are encountered in most submerged gas bubbling operations into liquid metals, and can be used to effectively, and efficiently, to stir up the metal bath. In fact, the operation of the old Open Hearth Furnaces, prior to the introduction of BOF steelmaking operations, relied on the "carbon boil". During this refining operation, the liquid iron bath, supersaturated with dissolved carbon and oxygen, would spontaneously form large spherically capped bubbles of carbon monoxide. These, in turn, would rise rapidly through the melt, so as to promote the necessary stirring reactions and associated mass transfer processes needed to remove carbon and other metalloids from the melt. In this way, the composition of a carbon saturated melt from the blast furnace, could be transformed into a liquid steel. Nonetheless, using large bubbles for stirring can have disruptive consequence. In many instances, for example, it will lead to generating dross as a result of large bubbles penetrating an upper aluminum metal interface, thereby promoting turbulence and entrainment of fragments of oxides protecting the metal surface. This leads to oxide entrainment, and dirtier metal.

In liquid aluminium systems, the SNIF degasser (Submerged Nozzle Injection Fluxing) system, and later gas injection systems, such as the ALPUR (Aluminum Purification) process (?), reduced natural bubble sizes forming, by using high speed rotor blades (SNIF), or rapidly rotating cylinders fitted with small exit holes, so as to generate smaller bubbles of Argon-Chlorine mixtures, through shearing mechanisms. These were effective. However, nowadays, these systems are being superseded by flux injection systems, which inject pure argon together with magnesium chloride

R.I.L. Guthrie · M.M. Isac (✉) · R.T. Ren
McGill Metals Processing Centre, 3610 University Street,
Montreal, H3A 0C5, Canada
e-mail: mmpc@mmpc.mcgill.ca

A.P. Ratvik (ed.), *Light Metals 2017*, The Minerals, Metals & Materials Series,
DOI 10.1007/978-3-319-51541-0_167

particles, versus argon-chlorine gas mixtures, so as to remove dissolved sodium, calcium and lithium, as salt particles from the aluminum coming from the Hall-Heroult Cells. For such systems, the flotation of salt micro-droplets following their reactions with dissolved Na, Ca, Li, by using micro-bubbles, might be very helpful. As such, the question of the necessary conditions for generating micro-bubbles in metallurgical systems remains a question that still needs to be answered, and more importantly, quantified.

Present Work

In the present work, we consider the flow of liquid aluminum from a holding furnace, emptying into a transfer launder, and from there, into a SNIF system. Alternatively, an equivalent flow in liquid steel would be the flow of liquid steel from a ladle through a ladle shroud, down into a tundish set below. In both cases, we have liquid metal, falling under gravity, from one vessel, into another, at speeds ranging from 0.5 to perhaps 10 m/s, maximum. The question is whether we can produce microbubbles in the down-comer tubes, connecting the two vessels? In order to address this issue, we decided to build a water model equivalent to such a system, and to measure bubble sizes accurately.

Experimental Equipment

The main objective of this research was to have a quantitative understanding of the mechanism of bubble generation under turbulent flow conditions in a ladle shroud, or equivalent flow system. The purpose was to be able to propose a universal optimal operation condition for bubble generation in ladle shroud applications. A highly schematic diagram of a (ladle shroud) vertical flow system, with the bubble measuring system set below, is presented in Fig. 1a.

As seen, a Turbine Water Flow Meter, plus a pressure gauge, were attached to the 21.0 mm diameter inlet pipe, located upstream of an aluminum slide gate nozzle. The dimensions were chosen so as to match the full scale water model tundish shroud, corresponding to RTIT's billet caster, located in SOREL, Quebec. Similarly, a Thermo Air Flow Meter was attached to the inlet ports, to prescribe the gas flowrate to a pre-selected orifice. Three sets of ladle shroud, fitted with 0.3, 0.5 and 1.0 mm diameter orifices, were built for this experiment. All ladle shroud models also had inner diameters of 21.0 mm. In each ladle shroud model, four orifices were precision drilled by laser, near the top region of the tube, which was attached to the bottom surface of the slide gate nozzle system

$$Slide\ Gate\ Opening\ Ratio = \frac{L_{overlap}}{D_{ladle\ shroud}} \times 100\%$$

Since the slide gate can alter the flow pattern of the water in the ladle shroud and vary the turbulence dissipation rate in the zone concerned, the slide gate opening ratio must be accurately controlled in order to quantitatively study the effects of the slide gate on sizes of bubbles generated. Once the ladle shroud model was installed, the water can only go through the overlap area as shown in Fig. 2a the overlap area, more commonly referred as the slide gate opening ratio, varies from 23.8% open to 61.9% open to 100% fully open. Similarly, we plot the Eotvos Number for our air-water system. It shows that all our small bubbles can be approximated as being roughly spherical, being $\sim$1 mm or less.

To measure bubble sizes, we used an inclined rectangular tank shown schematically in Fig. 1a. The inclined surface made it possible to accurately observe and measure a monolayer of bubbles, which is crucial in quantitatively investigating the afore-mentioned relationships. From experimental observations, the bubbles generated from the orifices tended to follow the water stream to enter the "tundish model", then hit and slide along the inclined acrylic glass wall for a short period of time. This provided an observation window to characterize the bubble size distributions by utilizing optical measurement techniques. Contrary to all other researchers [2–6] who have studied bubble generation in ladle shrouds, the present work characterizes bubble sizes experimentally. In a few cases, (e.g. Fig. 3a),

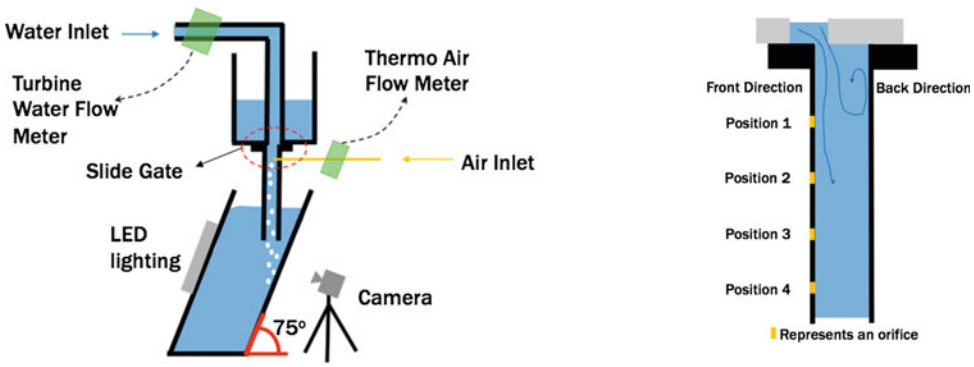

Fig. 1 **a** Experimental equipment for measuring bubble sizes forming in gas shroud/SEN systems. **b** Enlarged view of the ladle shroud with orifices. These were rotatable to 90,180, and 270° from the front direction

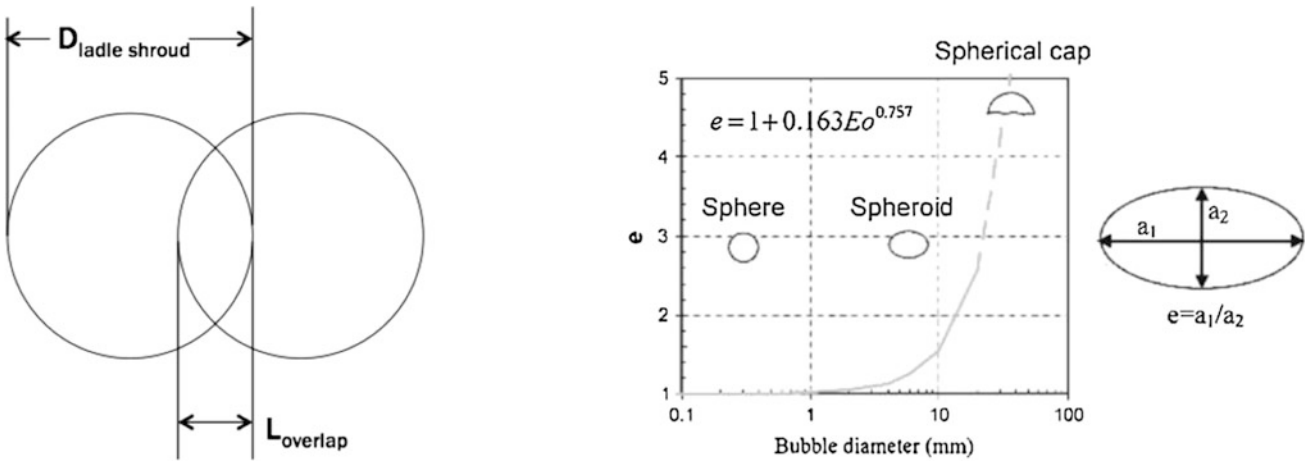

Fig. 2 **a** The slide gate had three fixed positions, fully open, 61.9% open, and 23.8% open, where the slide gate opening ratio was calculated, based on the equation: **b** Eotvos Number for bubbles versus Bubble Diameter

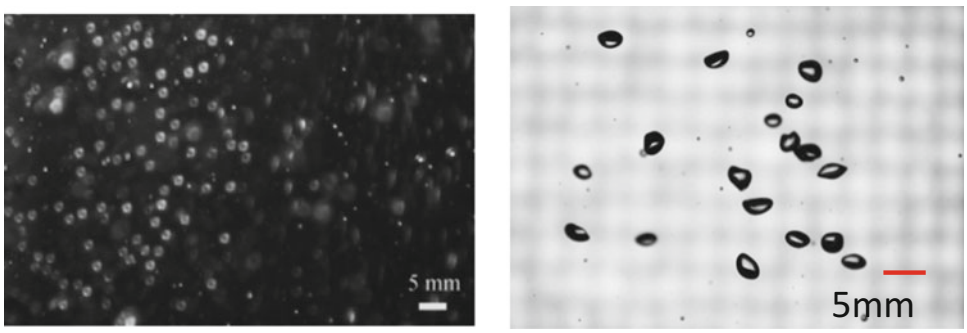

Fig. 3 **a** Previous report of a bubble cluster [6]. **b** A monolayer of bubbles located on the inclined sidewall

pictures of bubble swarms were presented to estimate bubble sizes but with very little justification. Thus, once implemented, the inclined surface of the tank in the present work (observe the monolayer of bubbles in sharp focus) was able to provide a drastic improvement in the quality of the bubble pictures, as shown in Fig. 4b. This innovation in measurement technique set the corner-stone to quantitatively analyze bubble generation mechanisms under turbulent conditions in a ladle shroud, or down coming tube, of equivalent geometry.

Thus, in the present water modelling experiments, the new water model that was built, was able to provide the possibility to quantitatively characterize the sizes of bubbles being generated. Six experimental factors were studied: (1) the water speed in the vertical flow tube, (2) the air injection rate, (3) the flow control valve (e.g. slide gate opening ratio), (4) the gas injection point distance from the control valve (or slide gate), (5) the direction of air injection and (6) the orifice size(s).

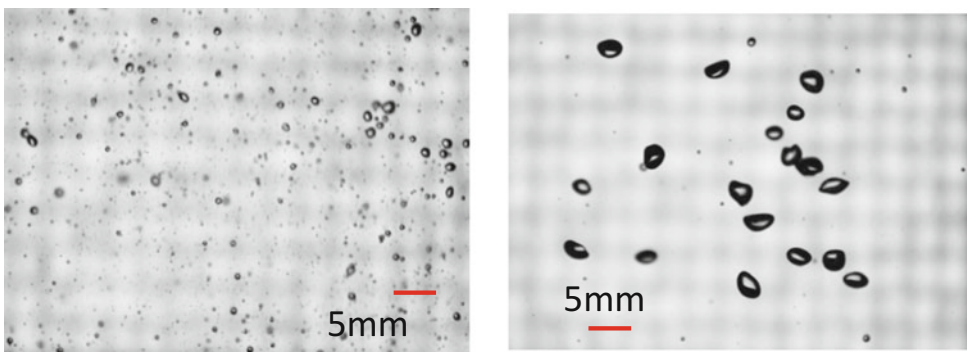

a b

Fig. 4 Two regimes of bubble formation: **a** small bubbles less than 1 mm formed when the water speed is high and the air injection rate is low; **b** big bubble more than 3 mm formed, when the water speed is low and the air injection rate is high

Optical measurement techniques were used in the experiments to characterize bubble size distributions. In order to achieve reliable and accurate experimental results, two factors must be met: 1, proper setting of camera and lighting: to get clear, sharp, well illuminated pictures of a monolayer of bubbles and 2, image processing: fine tuned image processing routines to analyze the pictures. A professional Digital Single-lens Reflex (DSLR) camera, model Canon 50D, was used to capture bubble images. This model is capable of taking photos with a maximum 4752 * 3168 pixel resolution with highest ISO (a measurement of the camera light sensitivity) of 3200 while the fastest shutter speed is 1/8000 s. In the experiment, the picture format was set as 'large' to get maximum resolution pictures. The ISO was set to 200 to avoid over-exposure and 'noise' in the pictures. The shutter speed used usually was in the range from 1/4000 to 1/5000 s. A professional photography level LED light was installed on the back of the inclined tank to provide consistent and bright lighting conditions. It is worth pointing out that when the experimental equipment is largely built using PMMA materials, high power light sources should be avoided, because the heat from high power light sources can easily build up and soften, or even melt, the PMMA (Poly-methyl methacrylate, commonly termed "acrylic glass").

Image Processing

In the first step, the program 'ImageJ' was used to process the pictures of bubbles taken from the experiments. For each set of experiments, one random picture would be chosen to fine-tune the process routine parameters. Once the parameter values were set, a macrocode was written (see Ren thesis) to batch process the set of images to record size of each bubble into a text file. In the second step, the text files would be imported into Excel to perform statistical analysis. Due to the extremely high volume of data from the text file, an Excel macrocode was also written to automate the importation and statistical analysis procedures. Finally, the processed data would be imported into a program called 'Origin' to produce graphs.

Visual Observations

First, two regimes of bubble formation were observed: (1) when the water speed was high (1.5 m/s) and the air injection rate was low (0.05 L/min), small bubbles were generated as shown in Fig. 4a. Most of these bubbles were less than 1 mm in diameter. (2) when the water speed was low (0.5 m/s) and the air injection rate was high (0.25 L/min), mostly big bubbles larger than 3 mm were generated from the ladle shroud as shown in Fig. 4b.

Water Speed Versus Bubble Size

Among the six controlling experimental factors, water speed was shown to have the strongest impact on the size of bubbles generated. In general, the higher the water speed in the ladle shroud model, the smaller were the bubbles generated. This trend is shown in Fig. 5. There, the three lines represent three

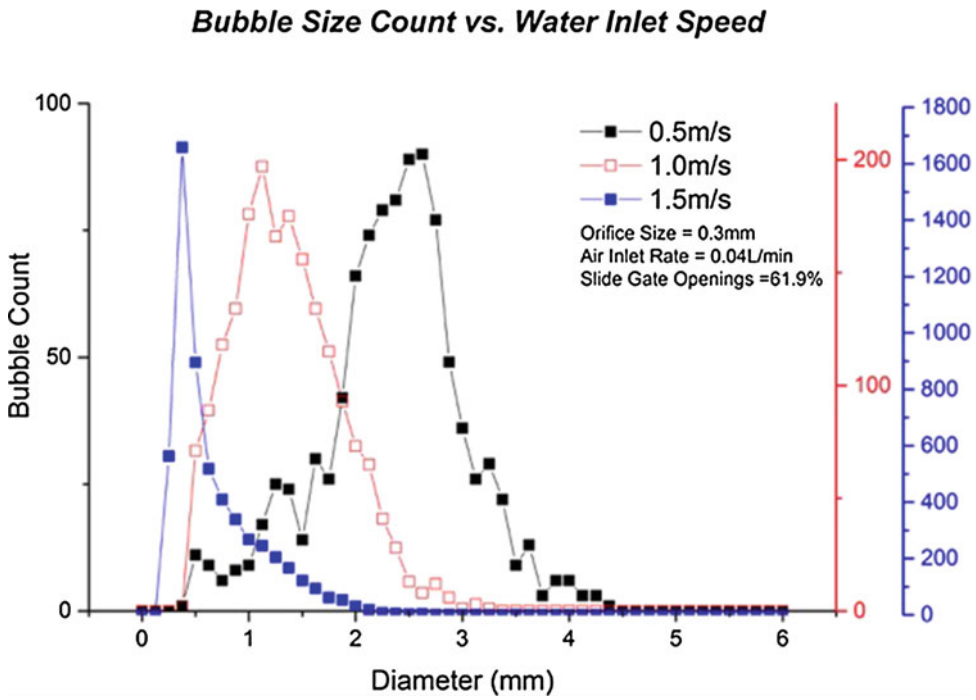

Fig. 5 Bubble size versus water inlet speed. Orifice size: 0.3 mm; Air inlet flowrate: 0.04 L/min; Slide gate opening ratio: 61.9%; Position 1

sets of experiments with identical conditions except the water inlet speed. The X-axis shows the bubble size in diameter (unit: mm), and all three Y-axes are bubble counts. It is clear that the bubble size peak shifts with water inlet speed. High water inlet speed (blue line: 1.5 m/s) has the bubble size peak around 0.5 mm; medium water speed (red line: 1.0 m/s) has the bubble size peak around 1.5 mm; low water speed (black line: 0.5 m/s) has bubble size peak around 2.5 mm. For a fixed air inlet rate (in this case it is 0.04 L/min), if individual bubbles were smaller, there would be more bubbles in total. This is why there are three Y-axes: when bubble size peak (blue line) was around 0.5 mm, the peak bubble count (blue Y-axis) went as high as 1800; when bubble size peak (red line) was around 1.5 mm, the peak bubble count (red Y-axis) dropped to 200; when bubble size peak (black line) was around 2.5 mm, the peak bubble count (black Y-axis) dropped below 100. If only one Y-axis was used, then the peaks of the red and the black line would not be seen.

Distance from the Slide Gate Versus Bubble Size

It can be shown from CFD results that the turbulence dissipation rate decays quickly down the tube. Four orifice positions were tested in the experiments to study the air injection point distance from the slide gate, close to the slide gate as possible in order to utilize the turbulence dissipation rate. As shown in Fig. 6, position 1 is 3 cm from the slide gate, 2 is 5 cm, 3 is 7 cm, and 4 is 9 cm away. Thus Fig. 6 summarizes related graphs for easier comparison purposes. Clearly the bubble size increases with the distance from the slide gate as the ball size (representing relative bubble sizes) increases from position 1 to 4. Therefore, the air injection point should be located as close to the slide gate as possible, in order to make use of the kinetic energy of turbulence in breaking down the sizes of bubbles forming, to even smaller sizes.

Summary of Experimental Results

The experimental results showed that the water speed and the slide gate opening ratio determined the critical bubble size of the system. A high water speed and a small slide gate opening ratio lead to smaller critical bubble sizes. In general, the bubble size increased with any increase in the air injection rate and in any increase in the distance of the gas injection point away from the slide gate. Therefore, the gas injection rate must be

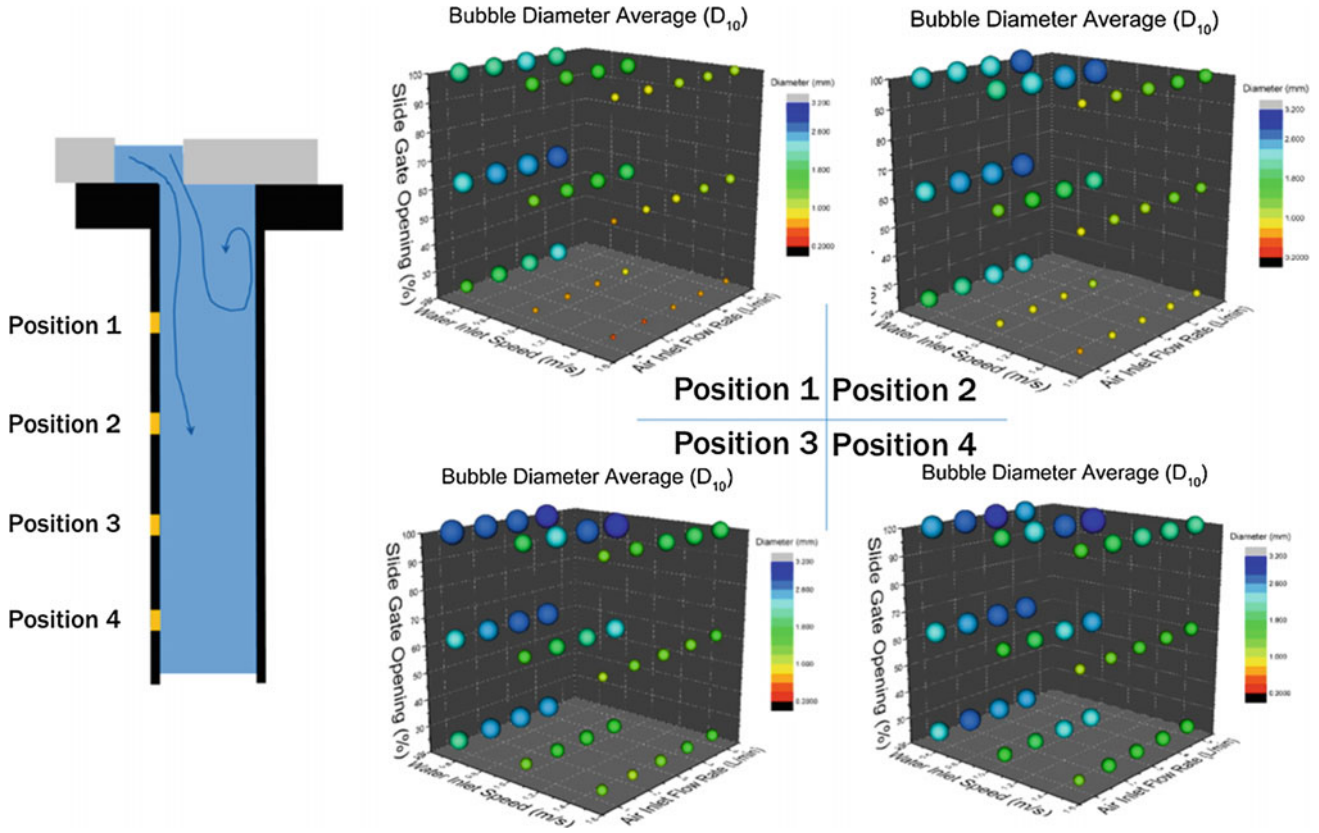

Fig. 6 Distance from the slide gate versus bubble size 0.5 mm Orifice size, front direction

kept low and the gas injection point should be located as close to the slide gate as possible, in order to generate very small bubbles. However, the direction of air injection and the orifice size did not show very strong correlations with the bubble sizes under the current experimental set-up and conditions. The smallest bubbles generated from the experiments were about 0.5 mm in diameter, which are predicted to be the optimum for removing small inclusions (10–50 μm) from liquid steel in a tundish, or small inclusions from liquid aluminum, flowing along a launder.

Computational Fluid Dynamic Simulations

In the CFD simulations, the commercial code package Ansys Fluent (version 14.5.7) was used. The simulations were carried out using the high performance computer in the McGill Metals Processing Centre (MMPC) at the Stinson laboratory. The simulation results, particularly the local turbulence dissipation rate values, were used to calculate the theoretical critical bubble sizes. The trajectories of bubbles of different sizes were studied using the so-called discrete phase model (DPM) in FLUENT-ANSYS. The results of the mathematical simulations were found to match the experimental results reasonably well.

Slide Gate Versus Bubble Size (CFD and Experimental Results)

The slide gate, when partially opened, can alter the local flow patterns significantly and create flow velocity gradients around the slide gate, as shown in Fig. 7. A high flow velocity gradient means high turbulence dissipation rates. As demonstrated experimentally, a "high" water speed (1.5 m/s) and high turbulence dissipation rates, can help generate smaller bubbles. In general, it was found that the smaller the slide gate opening ratio, the smaller were the bubbles generated.

Figure 7 presents an example of the CFD simulation results for a 23.8% slide gate opening ratio with an inlet water speed of 1.5 m/s. All the graphs produced (not shown here), focussed on the top 10% part of the ladle shroud model, where the gas injection orifices are located. The remaining 90% of the ladle shroud model was not presented because the flows had all practically reached steady state conditions by then.

Bubble Birth Size in a Cross Flow of Water

Marshall et al. [7] have proposed a semi-empirical relationship to predict the air bubble birth size, during bubbling

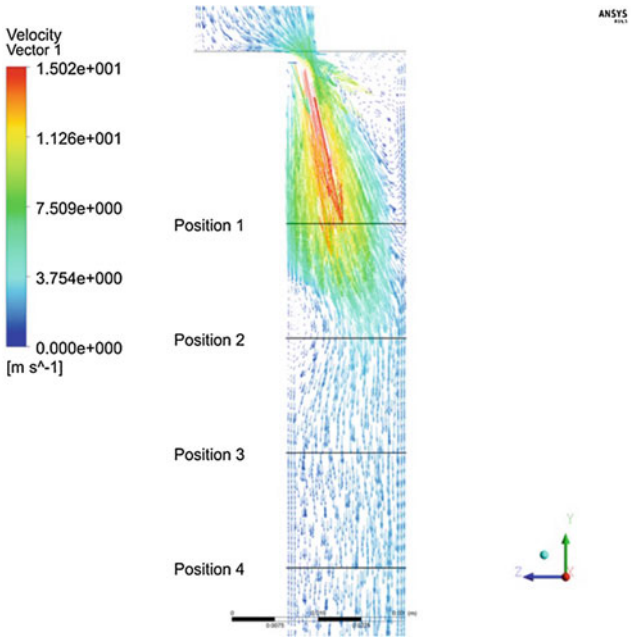

Fig. 7 Back flows and velocity gradients caused by a partially (quarter) opened slide gate nozzle

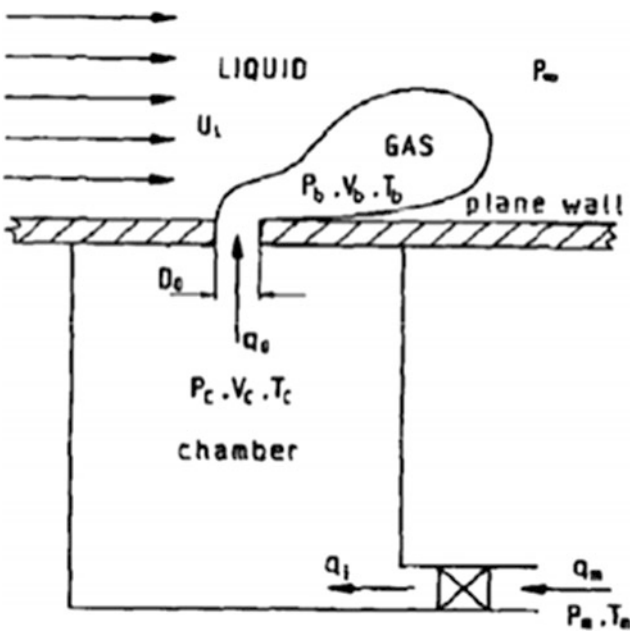

Fig. 8 Schematic of a flow of water across an orifice through which gas is being blown, generating bubbles

through an orifice into a horizontal cross-flow of water, as shown in Fig. 8.

The semi-empirical equation found for describing bubble birth radius was:

$$R_b = 0.48 R_{orifice}^{0.826} \left(\frac{U_{air}}{U_{Liquid}} \right)^{0.36} \quad \text{where} \quad (1)$$

$$U_{air} = Q_{air} / \pi R_{orifice}^2$$

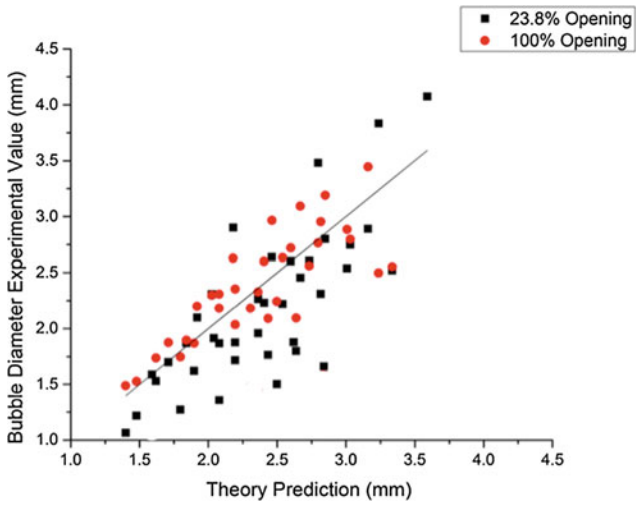

Fig. 9 Comparison of experimental bubble sizes versus predictions, using Eq. 1 for the cross flow of water in a tube into which gas could be injected

Here U_{air} is the superficial air inlet speed, and U_{liquid} is the speed of the cross flow of water in the tube.

Although their study was semi-empirical, the experimental conditions (orifice size, liquid velocity, air inlet rate) are very similar to the conditions carried out in the present research using water. Liu et al. [8] showed that the horizontal bubble formation mechanism (as used in Marshall et al. [7]) does not vary too much from the vertical bubble formation mechanism (i.e. the method used here). Therefore, it is reasonable to use this model to calculate the predicted birth size of bubbles, shown in Fig. 9. It is clear that for a fully-opened slide gate (red dots), where there are near zero velocity gradients and shearing flows, the data points fall nicely around the 1:1 line. This indicates the model from Marshall et al. [7] is suitable to estimate the birth sizes of bubbles generated in the absence of turbulent shear mechanisms. However, for a 23.8% slide gate opening (black dots), where there were usually strong velocity gradients with an accompanying high dissipation rate of the kinetic energy of turbulence, a large portion of the data points fall below the 1:1 line. This means the bubbles went through subsequent break-up processes after first being formed, owing to the dissipation of the kinetic energy of turbulence in skewed flow systems.

Conclusions

This work has laid the foundations needed for producing, and measuring, microbubbles sizes in liquid flow systems of interest to the metals industries. We show a methodology whereby both forming, and final, bubble sizes can be accurately measured and correlated against theoretical, or semi-empirical, data. The next step in this work will be to carry out equivalent flows in liquid metal/ceramic or refractory systems of interest, so as to confirm, or not, equivalence of results under the much higher surface tensions of liquid metal systems.

Finally, this work is dedicated to Professor Thorvald Engh, a good friend and colleague, who has devoted much of his life to the understanding of basic principles underlying industrial processing operations.

References

1. X.T. Ren, Bubble generation under turbulent conditions within a steelmaking ladle shroud: a water modeling and CFD study. PhD thesis, McGill University, Montreal, Canada (2015)
2. L. Wang, H.G. Lee, P. Hayes, A new approach to molten steel refining using fine gas bubbles. ISIJ Int. **36**(1), 17–24 (1996)
3. X. Zheng, P.C. Hayes, H.G. Lee, Particle removal from liquid phase using fine gas bubbles. ISIJ Int. **37**(11), 1091–1097 (1997)
4. J.S. Cho, H.G. Lee, Cold model study on inclusion removal from liquid steel using fine gas bubbles. ISIJ Int. **41**(2), 151–157 (2001)
5. J. Li et al., A new application of turbulator in removing inclusions by injecting gas from the shroud. Metalurgia Int. **17**(7), 57–62 (2012)
6. Q.Y. Zhang, L.T. Wang, Z.R. Xu, A new method of removing inclusions in molten steel by injecting gas from the shroud. ISIJ Int. **46**(8), 1177–1182 (2006)
7. S.H. Marshall, M.W. Chudacek, D.F. Bagster, A model for bubble formation from an orifice with liquid cross-flow. Chem. Eng. Sci. **48**(11), 2049–2059 (1993)
8. C. Liu et al., Effects of orifice orientation and gas-liquid flow pattern on initial bubble size. Chin. J. Chem. Eng. **21**(11), 1206–1215 (2013)